Color depth MIP mask search: a new tool to expedite Split-GAL4 creation

Hideo Otsuna[1*], Masayoshi Ito[1,2] and Takashi Kawase[1]

[1] Janelia Research Campus, HHMI, 19700 Helix Drive, Ashburn VA, 20147, U.S.A

[2] Institute of Molecular and Cellular Biosciences, The University of Tokyo, Yayoi, Bunkyo-ku, 113-0032 Tokyo, Japan

[*] Correspondence: otsunah@janelia.hhmi.org

Abstract:

The GAL4-UAS system has proven its versatility in studying the function and expression patterns of neurons the *Drosophila* central nervous system. Although the GAL4 system has been used for 25 years, recent genetic intersectional tools have enabled genetic targeting of very small numbers of neurons aiding in the understanding of their function. This split-GAL4 system is extremely powerful for studying neuronal morphology and the neural basis of animal behavior. However, choosing lines to intersect that have overlapping patterns restricted to one to a few neurons has been cumbersome. This challenge is now growing as the collections of GAL4 driver lines has increased. Here we present a new method and software plug-in for Fiji to dramatically improve the speed of querying large databases of potential lines to intersect and aid in the split-GAL4 creation. We also provide pre-computed datasets for the Janelia GAL4 (5,738 lines) and VT GAL4 (7,429 lines) of the Drosophila central nervous system (CNS). The tool reduced our split-GAL4 creation effort dramatically.

Introduction:

Genetic targeting and control of defined sets of neurons in transgenic animals has accelerated our understanding of the morphology and function of the nervous system in many animals. This has been especially apparent in the fruit fly, *Drosophila melanogaster.* In flies, the GAL4-UAS system is a robust method for targeting gene expression into specific neurons (Brand and Perrimon, 1993; Jenett et al., 2012; Pfeiffer et al., 2008) . Many large collections of GAL4 driver lines are publically available (Dionne et al., 2018; Jenett et al., 2012; Pfeiffer et al., 2008; Tirian and Dickson, 2017; http://flweb.janelia.org/cgi-bin/flew.cgi), and although these collections have yielded many new insights into the neural basis of behavior (Otsuna et al., 2014; Robie et al., 2017) the pattern of neuronal expression remains broad in these lines making it difficult to ascribe function to individual cells. Further refinement of the expression patterns is possible using the split-GAL4 system is used to eliminate unnecessary GAL4 expression from the out of target neurons and achieve individual cell-type specificity (Luan et al., 2006).

To achieve this specificity, activation domain (AD) and DNA binding domain (DBD) hemidriver 'split-halves' that are derived from GAL4 patterns are combined and drive the expression of the GAL4 system only in overlapping cells (for a detailed review see Dionne et al., 2018). This intersectional approach to generating split-GAL4 driver lines is a powerful tool in Drosophila neurobiology (Aso et al., 2014; Namiki et al., 2017; Wu et al., 2016), but the screening of confocal stacks in 3D to find overlapping neurons from more than ten thousand of GAL4 lines is an onerous task on the part of the researcher. Here we present a novel way to rapidly query the expression patterns of thousands of driver lines and computationally determine which lines likely contain a neuron or set of neurons of interest. We do this by first generating maximum intensity projection images (MIPs) where color represents the depth.

Thus, the neuron searching method for the split-GAL4 creation is ideal due to the following characteristics: it is non-segmentation based, the original x-y resolution is maintained, it not only queries for neurons but also can provide other neuronal expression levels, the original brightness of the neurons is reflected, there is an easily modified 3D mask, and the ease of adding additional datasets into the searching data. Therefore, this searching method is not just for individual neurons, but can query entire expression patterns as seen in GAL4 driver lines.

Here are our results for the new 3D neuron searching method for the split-GAL4 creation from original GAL4 expressed data.

Results:

Our searching method creates a matching score from the overlapped pixel number of color depth MIP (Timo et al,, 2006). The pixel color represents z-depth. The xy resolution is same as the JFRC2010 template. If the color and xy position of the pixel match between the mask and the searching data, then the approach here will count it as a positive matching score. The matching color range can be set to certain fluctuation; this will adjust for alignment errors and individual brain/neuronal shape difference between samples. Unlike the skeleton, our non-segmentation based searching method can use the original thickness of the neurons. Typically, a single neuron has around 5 pixel thickness in our JFRC2010 aligned brain. This thickness also adjusts for neuronal position difference between samples.

Workflow:

Original confocal stacks need to be aligned to a single 3D template. Then the color depth MIPs are generated from each of aligned stacks individually (Fig. 1A-D). If there are the same neurons in different samples; the MIP color of the neurons became almost identical after the alignment step. To search for a neuron of interest, the user can create a mask by using the freehand tool in Fiji (Fig. 1E). The search is

performed against the color MIP dataset; the positive hit is usually 0.5~2% of the original dataset (Fig.1 F).

Automatic-brightness adjustment:

Before the MIP creation, our program adjusts the image brightness automatically for enhancing the neuron searching sensitivity. To set neuronal brightness equally between different brains, we create the mask for the neuron fibers only but not for the cell bodies/tick neuron bundles (Fig. 2A, B). We employed the 2D rod shape neuronal segmentation fitting method to the neuronal fiber segmentation - Direction selective local thresholding (DSLT) (Kawase et al., 2015). The method allows us to avoid the intensity measuring of the bright bold structures. The adjusted brightness is for fine neuronal fibers. Our program adjusts averaged pixel value to desired brightness value (usually 190~200 /255 gray value) within the 2D mask. The dimmer signal becomes brighter after using high-thresholding of the gray value. Though that approach, the user can tell the brightness of the sample from this thresholding value. The dimmer samples require more brightness enhancement with lower thresholding value. But the images from different brains will look the same for brightness (Fig 2C, C', D).

Z-depth Color MIP creation:

For the accurate single slice z-resolution and the easy visual screening of the results, we created new color look-up-table (LUT) (Fig. 2E). We also modified the method of MIP creation to keep the accurate z-depth information in the MIP (Fig. 2F). The color matching algorithm is based on our LUT. Our method counts only the top two gray values among three of RGB channels for the color matching. The highest gray value represents original gray value. The ratio between 1st and 2nd top gray values represents the z-slice number. If the 3rd gray value is lower then the 2nd gray value, then the highest 3rd value will be accepted as a MIP signal. We found that the 3rd value enhanced the visual screening efficiency (Fig. 2G).

Mask creation:

The screening process requires quick 3D mask creation and quick result image browsing. We implemented the program in Fiji (https://fiji.sc/). The user can create mask from either 3D segmented neuron or the color depth MIP image. If the former method is applied, we have been developing branch out version of the FluoRender software (Wan et al., 2009), VVDviewer (https://github.com/takashi310/VVD_Viewer). The software provides the user with quick 3D segmentation on the 2D display. If the latter method is applied, the user can use the Fiji's 2D ROI creation function (Polygon/Freehand selections). Either way, the 3D mask creation will only need a few minutes.

Searching algorithm and speed

Color matching algorithm between the mask and the searching data are in Fig. 2G. The pixel from mask: pix1, the pixel from the data: pix2. Both pixels create "two color ratio" from the highest color value (1st value) and 2nd color value. Center of the images: The color depth MIP mask search plugin compares between these two color ratios. Higher color fluctuation setting will accept wider differences between the ratios: it allows the color matching between more z-depth shifting, as well as x-y displacements of up to 4 pixels to compensate for differences in alignment between samples.

The overlap search is performed only within the mask area. Thus, the searching is efficient and fast. If the user loads images from SSD performance is ~15 seconds for 8,000 samples 11.7GB, ~30-45 seconds from the HDD, ~7 seconds from the system memory.

Reviewing search results

We also found that the reviewing process of searching result is critical in the workflow. If the user needs to spend time more than few seconds per image, it is not intuitive. For example, the original searching images are ~46,445, then the mask

search will narrow down to ~1% (200~500) of images. Usually, the user needs to check top 50~150 images. Our color depth MIP visualization allows the user to check the 50~150 images within ~10 minute. Color depth MIP mask search method itself could not hit the line if the targeted neuron is covered by the cloud of neurons. This feature matches to both of the AD/DBD split-GAL4 picking and the reviewing process.

Comparison with NBLAST

For adding new aligned data to an exiting database, NBLAST (Costa et al., 2016) needs 3D segmentation and conversion to the vector data by using R coding. It then needs to associate the NBLAST data and GAL4 line MIPs in order to make it effective for the split-GAL4 to be picked-up. However, in our color depth MIP method, users only need to create the MIP and move the file into an existing MIP set folder. Unlike other searching databases, the color depth MIP searching method is searching the original GAL4 image itself. It does not require linking to the image and searching query.

Search results:

We compared the search results by using ~3500 of Janelia GAL4 lines (http://flweb.janelia.org/cgi-bin/flew.cgi). We used three dataset for our comparison: this Color depth MIP, the NBLAST dataset from VirtualFlyBrain (VFB) and the NBLAST dataset with newly DSLT segmentation. The NBLAST data from the VFB missed many of neurons (Fig. 3B). Thus, we re-aligned the Janelia Gen1 GAL4 lines and newly 3D segmented GAL4 expressed neurons by the DSLT high-sensitive 3D segmentation method (Fig. 3C). Then we created the new NBLAST database. This new dataset contains many more segmented neurons than the VirtualFlyBrain's dataset. The test searching masks are generated from previously published split-GAL4 lines (http://splitgal4.janelia.org/cgi-bin/splitgal4.cgi, R_MB027B, R_OL0001B (LC22), R_OL0015B (LC11), SS0732, SS4159 (Aso et al., 2014; Shigehiro Namiki, 2017; Wu et al., 2016). We choose three different neuronal shape characters

for the searching test. Bold bright fiber: R_MB027B, tick fascicle lobula columnar neuron: R_OL0001B (LC22), R_OL0015B (LC11) (Otsuna and Ito, 2006), fine neuro-fiber: SS0732, SS4159.

In our test, NBLAST tends to hit high-density GAL4 expressed line (Table 7 K-N, Table 8 H-N). These high-density GAL4 expressed lines are not desirable for the split-GAL4 creation. The NBLAST matching score is a result of the local point vector matching. Surrounding neurons could increase matching score (Fig. 3E, F). Thus, our new high-sensitive segmented NBLAST dataset ranked the specific GAL4 expressed lines lower than the high-density GAL4 expressed lines (Tables 1, 3, 4, 5).

NBLAST dataset from the VFB worked well only with the mushroom body output neurons from the R_MB027B split line within the five neurons test. The neuron was bright and bold. It was segmented nicely in many cases. However, both of the lobula columnar neurons were not detected well by the NBLAST VFB (Table 2, 3), because the segmentation of the lobula are often lacking. This is the reason of the NBLAST DSLT containing more hits than the NBLAST VFB of the lobula columnar neurons (Table 2, 3). However, The NBLAST DSLT was too sensitive to any of the lobula columnar neurons. Therefore, the real hits are spread within top 50 ranking (Table 3) and less number of real hit (Table 2). The lack of segmentation of the NBLAST VFB is also observed in Table 4 and 5. In Table 4, NBLAST VFB could not hit R_14F03 (AD) line within top 50, due to the lack of segmentation (Fig. 3A-C).

The color depth MIP searching method could hit more useful samples for the split-GAL4 creation than the NBLAST VFB and NBLAST DSLT with both the fine fibers and bold LC neurons in our test (Table 6 - 10). For example, in Table 8, B-G are hit only by the color depth MIP searching, H-N are only hit by the NBLAST searching at more than top 50 ranks. The relatively specific LC11 GAL4 expression is in B, C, D, F, G but not in H, I, K, L, M, N.

The high-sensitivity of the color depth MIP searching is based on the automatic brightness adjustment. For example, for line SS00732 the AD line (14F03, 665/4095 brightness increased, Table 6F) and the DBD line (24C07, 271/4095 brightness, Table 6D) are both so dim for the original GAL4 expression. Their brightness is increased significantly during the MIP creation.

Resources from this study:

The 46,445 color depth GAL4 brain MIPs from the Gen1-R GAL4 (5,738 lines) and VT GAL4 (7429 lines). The 9,395 of LexA brain MIPs from the Janelia Gen1-LexA (1,100 lines) and VT LexA (2020 lines). The 15,057 of GAL4 VNC MIPs from the Janelia Gen1-GAL4 (7,491 lines) and VT GAL4 (2795 lines). The 3,534 of LexA VNC MIPs from the Janelia Gen1-LexA (1,536 lines) and VT LexA (1,497 lines). The pre-computed color depth MIPs links to the source code can be found at: https://www.janelia.org/open-science/color-depth-mip

The Fiji based color depth MIP searching program is in this location (https://github.com/JaneliaSciComp/ColorMIP_Mask_Search). VVDviewer: 3D/4D visualization and 3D segmentation software (https://github.com/takashi310/VVD_Viewer).

Discussion:

From the searching test of the color depth MIP method, we could hit all of AD/DBD split pairs for all five split-GAL4 lines. (Split-GAL4 line: SS00732, R24C07 (DBD) is not in the NBLAST VFB dataset. However, when we added the color depth MIP to the searching dataset, it was found as the 40th highest hit (Data not shown). This result suggests that our searching method is useful for split-GAL4 creation. Also, we have internally validated using the the color depth MIP method in multiple visitor projects and labs in Janelia (https://www.janelia.org/you-janelia/visiting-scientists/active-projects: 1) Generation of cell-type-specific GAL4 driver lines for neurons of the Drosophila adult leg neuropil; 2) Whole Fly Brain Tracing Effort: The Lobula Plate Tangential cells: elucidating the feed-forward and feedback circuitry; 3) Generation of cell-type specific GAL4 driver lines for neurons in the Drosophila adult flight and haltere neuropil of the ventral nerve cord; 4) Mapping and analyzing neurons in the terra incognita regions of the Drosophila brain; 5) Mapping the lateral horn of Drosophila; 6) Generation of cell-type specific GAL4 driver lines for neurons in the Drosophila adult suboesophageal ganglion; 7) Development of Hemilineage Tools for Studying Neurons of the Adult Drosophila CNS; 8) Genetic dissection of somatosensory neural circuits in the Drosophila ventral nerve cord). Our method is extremely useful for picking AD/DBD pairs from more than 46,445 Gen1 GAL4 images. Multiple researches can pick up ~90% of AD/DBD pairs that likely target the neuron(s) of interest. Then they could create split-GAL4 lines around 60~80% of the whole known neuron type (results will be published in future), though the individual success rate for a given intersection typically is in the 10-30% range as detailed in Dionne et al., 2018.

In order to accelerate neuron seaching in large datasets, the NBLAST and Braingazer programs were introduced (Bruckner et al., 2009; Costa et al., 2016). Though these tools are very valuable for specific applications, in our hands these methods weren't well suited for split-GAL4 line creation. The split-GAL4 system requires identifying

specific expression patterns in overlapping parental driver lines that have little to no overlap of off target neurons. Neither of these methods is accounts for other expression within the GAL4 line potentially leading to non-specific split-GAL4 expression. In addition, both methods require 3D neuronal segmentation to enable searching. Segmentation of high-density GAL4 expression patterns is challenging. Moreover, split-GAL4 driver lines are often better produced from strongly expressed parental lines. Previous methods do not account for the brightness, and thus expression level, of the neurons. Current NBLAST databases rely on skeletonization don't account for the thickness of fascicles. If the mask is a single neuron, and target is a thick neuronal fascicle with a different shape, NBLAST has problems with detection. Since searching the GAL4 dataset is not a single neuron, the user often needs to modify the 3D mask to pick the targeted neuron. The 3D mask modification is also another challenge in NBLAST but not in Braingazer. However, Braingazer's database provides averaged signals from three different aligned brains, which means fine fibers are easily missed from the database.

Through the analysis of mask search results, we found that many neurons have relatively high shape fluctuations in the neuronal trunk and location of the cell body, but not in the projections. Some neurons exhibit remarkable stability, especially those that aggregate in tracts. These stable characteristics are useful to produce high hit rates. Some neurons are easy to target, but some are not. So, if the neuron has high stable character, it is relatively easy to hit.

We analyzed the alignment fluctuations in the Janelia Gen1 GAL4 collection and found that neurons are usually within ~5 px in the JFRC2010 template resolution (1024 x 512 px). Since most neurons are 3~5 px thick, the alignment fluctuation is within the range of neuron fiber thickness. But if we use skeletonized neurons for searching, the alignment variability will be a challenge.

In order to eliminate high density GAL4 expressed lines, our color depth MIP method allows the user to skip pre-calculation of the density of expression from

many brain areas. The MIP itself shows the strongest GAL4 expressed neurons as a result. MIP generation will not render the targeted neuron if the expression pattern around the targeted neuron is too dense, thus excluding patterns that are too dense. Therefore the result of the color depth MIP search contains more specific GAL4 lines, meaning the color depth MIP searching method is very useful for split-GAL4 AD/DBD selection.

Method:

We used aligned confocal images of the Janelia and VT GAL4 collections (Jenett et al., 2012; Pfeiffer et al., 2008; Tirian and Dickson, 2017) to generate color depth MIPs. The Janelia and ~3000 of VT brain images and VNCs were imaged by the FlyLight project team (https://www.janelia.org/project-team/flylight). The rest of the VT brain images were imaged in Vienna (Tirian and Dickson, 2017) . The Janelia collection brains were aligned by JBA and CMTK (Peng et al., 2011; Rohlfing and Maurer, 2003). VT brains are aligned by Amira software then transformed to JFRC2010 template space by CMTK. The color depth MIPs are created by our new program based on Fiji (https://fiji.sc/) https://www.janelia.org/open-science/color-depth-mip. All of the VNC (15,057 of Gen1-GAL4 and 3,534 of LexA) are imaged by the FlyLight project. All VNC are aligned by our newly coded VNC global aligner + CMTK.

Acknowledgement

We thank Gerry Rubin, Barry Dickson and the other members of the FlyLight steering committee for supporting the Color MIP tool development and VNC aligner. Wyatt Korff and Robert Svirskas for the editing and discussion of the manuscript. We thank Robert Court for an early version and inspiration for the VNC aligner. The FlyLight Project Team for the generation of original confocal files. Sean Murphy for encouragement during this project.

Figure 1. Workflow. **A-C:** Original confocal stacks need to be aligned to a single 3D template. **D:** The color depth MIP is generated from the aligned stacks. **E:** Example of a searching neuron. **F:** example of searching dataset and the results. The search results contain the target neuron as a positive hit.

Figure 2. Color depth MIP creation and the mask search algorithm. **A-B:** The mask creation for the brightness measurement of neuron fibers. **A:** Original MIP signal, **B:** Direction sensitive local threshold (DSLT) mask. The mask skips bold and bright structures (Arrow: the elipsoid body). Thus, the measured brightness is mainly from the neuron fibers. **C-D:** Example of the auto-brightness adjustment. **C:** Original image of the R58F07 line. The GAL4 expression is too weak and could not show the neuro-fibers. **C':** Auto-re-mapped the gray scale value 20 as 255 from the C. **D:** The strong GAL4 expression line R69F02, the brightness of the image is original value. C' and D are almost similar brightness. **E:** Color look up table of our color depth MIP. Y axis is the brightness of the signal. X axis is Z-slice number. One of the RGB channels represents original gray scale value (Top line, 1st value). The ratio between 1st and 2nd color value represents unique Z-slice number within the 255. **F:** The MIP method comparison between normal MIP and our MIP. In the normal MIP (left panel), the RGB signals between different slices are independent. Just the maximum value of each RGB will create the MIP. The MIP will create the 1st value (R-170) and the 2nd value (G-150) pair. The pair does not exist within the z-stack. In our MIP (right panel), the 1st value and the 2nd value are paired from a single slice. **G:** Color matching algorithm between the mask and the searching data.

Figure 3. The analysis of neuron search results. **A:** Aimed neuron SS00732 split-GAL4 line, **B:** The color MIP of R14F03 GAL4 line. The line was used as AD line. The color MIP mask search hits this line as rank #23 and the R24C07 (DBD) line as rank #4. **C:** NBLAST VFB could not hit the R14F03 line due to lack of the segmentation (Yellow arrow head). But it hits R24C07 as rank #3. **D:** NBLAST DSLT hits the R14F03 line as rank #17 but could not hit the R24C07 line within the top 50. **E-F:** Top score GAL4 line R78A10 in the NBLAST DSLT. The line has too much GAL4

expression. It appears to be false hit. In fact, it is due to increase score by high density of other fibers. It is difficult to tell if this is real hit or not. **E:** Original GAL4 expression. The yellow rectangle area in F. Yellow circle is the position of mushroom body peduncles. **F:** Green: local vector, White: Submitted skeleton. Arrow head (1): The area has dense arborization from other neurons. some local vectors are matching with SS00732 neuron. (2): local vectors are not existing in the trunk, (3): the vertical line is the cell body fiber. Many other neurons have cell body fiber in the area.

Table 1-5. Searching results of a neuron from the stable split-GAL4 line. The tables are the top 50 hits from multiple search methods: from the left, Color depth MIP search, NBLAST data from virtual fly brain, NBLAST data from our high-sensitive DSLT segmentation. All searching methods have the same Janelia GAL4 dataset. In the table, yellow cell represents real hit of the neuron. The yellow cell + red character represents original AD/DBD line. A: The searched neuron from the split-GAL4 line. B: The GAL4 line image used as AD. C: The GAL4 line image used as DBD.

Table 6-10. The comparison among the positive hits from three-searching methods. A: The neuron used as searching mask from the original split-GAL4 line. B-N: The positive hits GAL4 images that contain the neuron from split-GAL4 lines. C#: hits by color depth MIP search, the number is ranking. V#: hits by NBLAST search by using virtual fly brain data. D#: NBLAST search hits by using DSLT segmented data.

References

Aso, Y., Hattori, D., Yu, Y., Johnston, R.M., Iyer, N.A., Ngo, T.T., Dionne, H., Abbott, L.F., Axel, R., Tanimoto, H., *et al.* (2014). The neuronal architecture of the mushroom body provides a logic for associative learning. Elife *3*, e04577.

Brand, A.H., and Perrimon, N. (1993). Targeted gene expression as a means of altering cell fates and generating dominant phenotypes. Development *118*, 401-415.

Bruckner, S., Solteszova, V., Groller, M.E., Hladuvka, J., Buhler, K., Yu, J.Y., and Dickson, B.J. (2009). BrainGazer--visual queries for neurobiology research. IEEE Trans Vis Comput Graph *15*, 1497-1504.

Costa, M., Manton, J.D., Ostrovsky, A.D., Prohaska, S., and Jefferis, G.S. (2016). NBLAST: Rapid, Sensitive Comparison of Neuronal Structure and Construction of Neuron Family Databases. Neuron *91*, 293-311.

Dionne, H., Hibbard, K.L., Cavallaro, A., Kao, J.C., and Rubin, G.M. (2018). Genetic Reagents for Making Split-GAL4 Lines in Drosophila. Genetics *209*, 31-35.

Jenett, A., Rubin, G.M., Ngo, T.T., Shepherd, D., Murphy, C., Dionne, H., Pfeiffer, B.D., Cavallaro, A., Hall, D., Jeter, J., *et al.* (2012). A GAL4-driver line resource for Drosophila neurobiology. Cell Rep *2*, 991-1001.

Kawase, T., Sugano, S.S., Shimada, T., and Hara-Nishimura, I. (2015). A direction-selective local-thresholding method, DSLT, in combination with a dye-based method for automated three-dimensional segmentation of cells and airspaces in developing leaves. Plant J *81*, 357-366.

Tirian L. and Dickson B . (2017). The VT GAL4, LexA, and split-GAL4 driver line collections for targeted expression in the Drosophila nervous system. bioRxiv.

Luan, H., Peabody, N.C., Vinson, C.R., and White, B.H. (2006). Refined spatial manipulation of neuronal function by combinatorial restriction of transgene expression. Neuron *52*, 425-436.

Otsuna, H., and Ito, K. (2006). Systematic analysis of the visual projection neurons of Drosophila melanogaster. I. Lobula-specific pathways. J Comp Neurol *497*, 928-958.

Otsuna, H., Shinomiya, K., and Ito, K. (2014). Parallel neural pathways in higher visual centers of the Drosophila brain that mediate wavelength-specific behavior. Front Neural Circuits *8*, 8.

Peng, H., Chung, P., Long, F., Qu, L., Jenett, A., Seeds, A.M., Myers, E.W., and Simpson, J.H. (2011). BrainAligner: 3D registration atlases of Drosophila brains. Nat Methods *8*, 493-500.

Pfeiffer, B.D., Jenett, A., Hammonds, A.S., Ngo, T.T., Misra, S., Murphy, C., Scully, A., Carlson, J.W., Wan, K.H., Laverty, T.R.*, et al.* (2008). Tools for neuroanatomy and neurogenetics in Drosophila. Proc Natl Acad Sci U S A *105*, 9715-9720.

Robie, A.A., Hirokawa, J., Edwards, A.W., Umayam, L.A., Lee, A., Phillips, M.L., Card, G.M., Korff, W., Rubin, G.M., Simpson, J.H.*, et al.* (2017). Mapping the Neural Substrates of Behavior. Cell *170*, 393-406 e328.

Rohlfing, T., and Maurer, C.R., Jr. (2003). Nonrigid image registration in shared-memory multiprocessor environments with application to brains, breasts, and bees. IEEE Trans Inf Technol Biomed *7*, 16-25.

Namiki S., Dickinson M. H., Wong, A. M., Korff W., Card G. M. (2017). The functional organization of descending sensory-motor pathways in Drosophila. bioRxiv.

Timo R, Frank S, and Klaus H (2006). Visually Supporting Depth Perception in Angiography Imaging. International Symposium on Smart Graphics SG 2006: Smart Graphics pp 93-104 *4073*.

Wan, Y., Otsuna, H., Chien, C.B., and Hansen, C. (2009). An interactive visualization tool for multi-channel confocal microscopy data in neurobiology research. IEEE Trans Vis Comput Graph *15*, 1489-1496.

Wu, M., Nern, A., Williamson, W.R., Morimoto, M.M., Reiser, M.B., Card, G.M., and Rubin, G.M. (2016). Visual projection neurons in the Drosophila lobula link feature detection to distinct behavioral programs. Elife *5*.

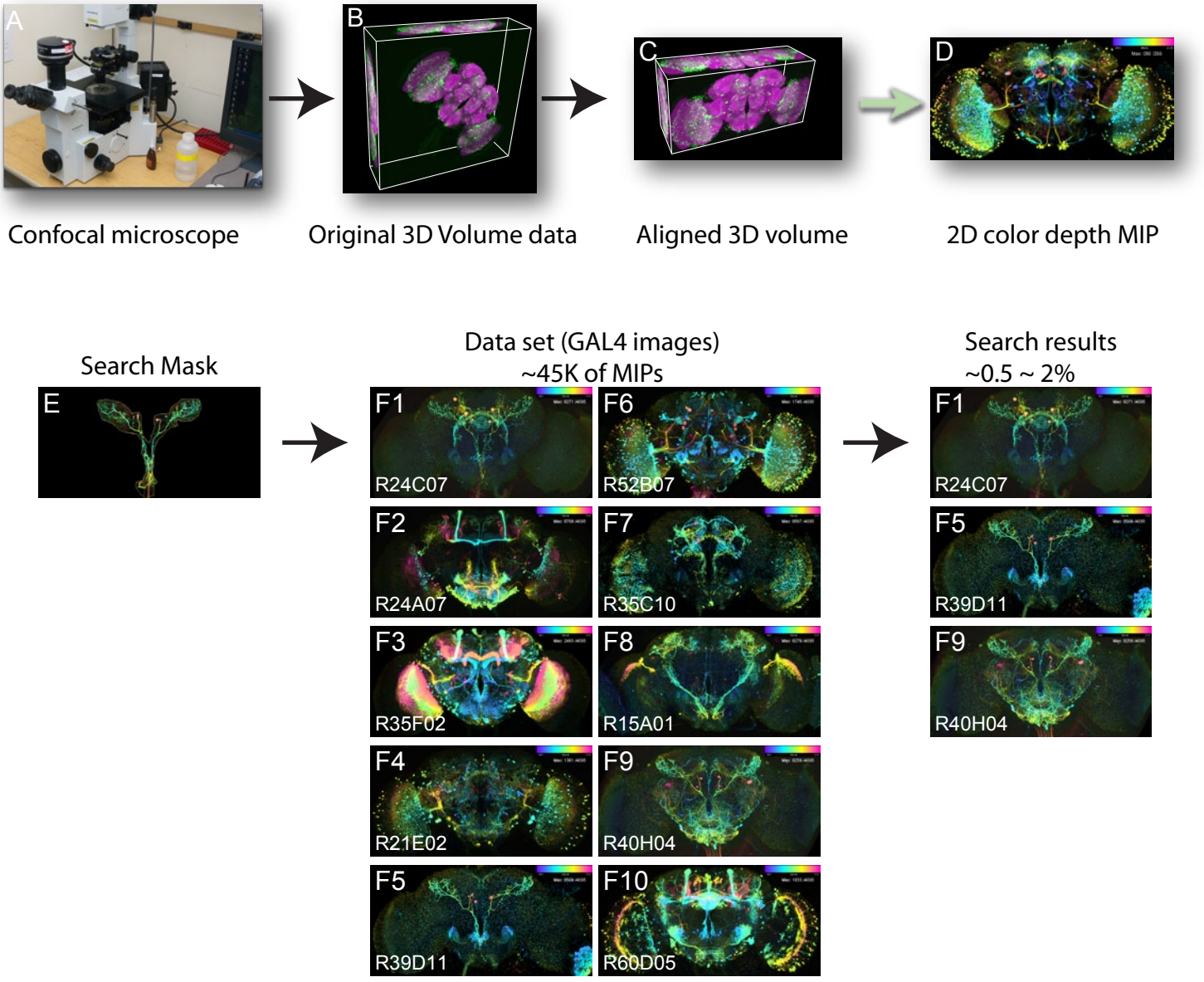

Figure 1

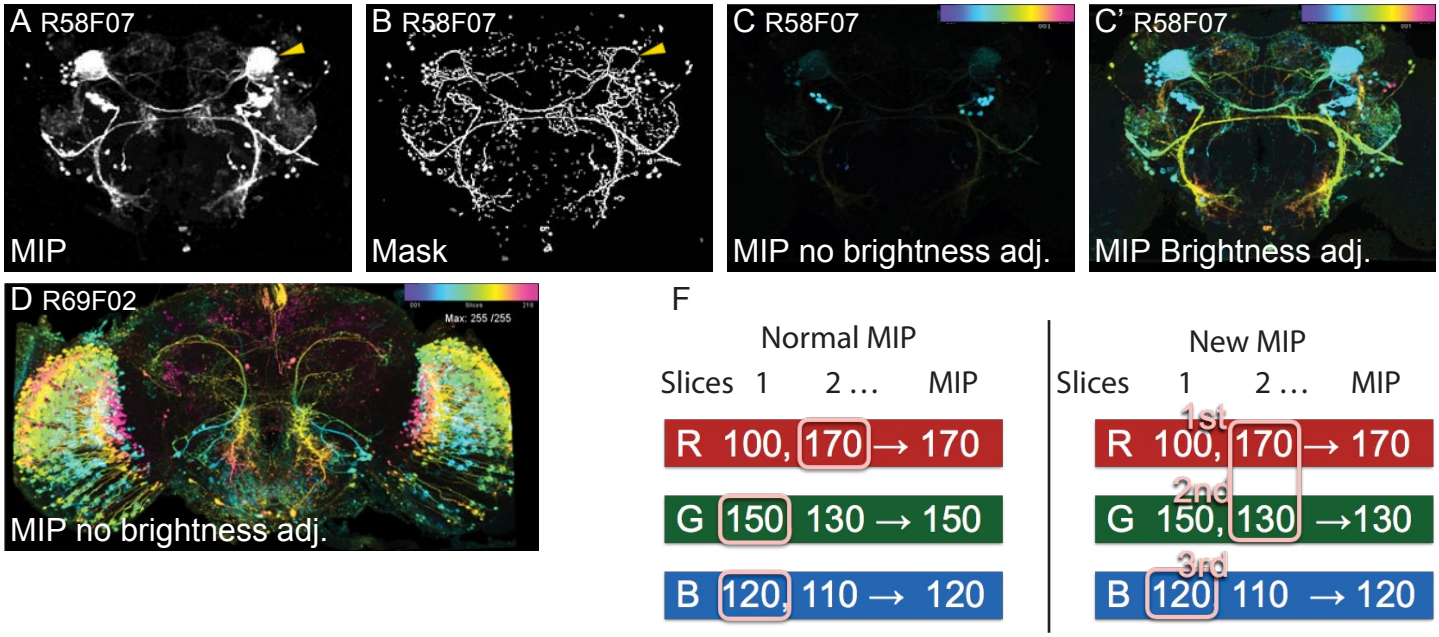

Figure 2

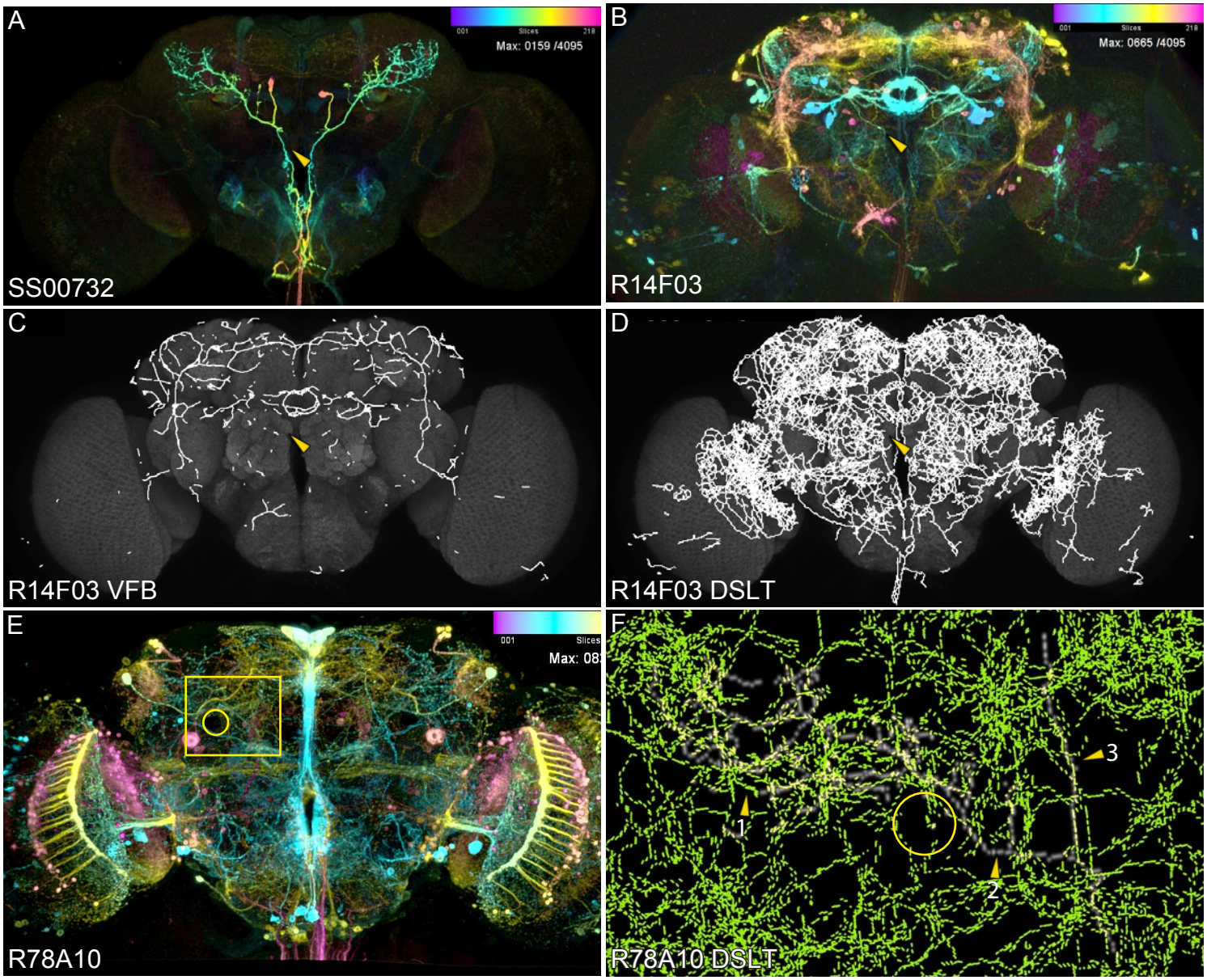

Figure 3.

R_MB027B_AD_R24H08_DBD_R53F03

	ColorMIP (16)		N-VFB (13)		N-DSLT (10)
	Line		Line		Line
1	R53B06		R42D11		R76B02
2	R42D11		R53B06		R42D11
3	R39H01		R49A11		R34H05
4	R53F03		R38D01		R93G02
5	R93G02		R33E02		R39C07
6	R34H05		R24H08		R91B03
7	R24H08		R93G02		R48G10
8	R38D01		R53F03		R11F08
9	R33E02		R74B10		R93C09
10	R15H10		R20G01		R33E02
11	R41F07		R93G06		R58D11
12	R84A06		R39H01		R88H09
13	R91A03		R34H05		R50F02
14	R92B01		R82H06		R53F03
15	R65C03		R70F10		R47A10
16	R26F01		R34D03		R91H05
17	R41E08		R91H05		R30B10
18	R93G06		R78F03		R49C12
19	R18F04		R89D06		R76H04
20	R49A11		R83C05		R83C05
21	R76H04		R16C09		R92B02
22	R81E11		R21B06		R85F05
23	R82F06		R33D07		R93F03
24	R30B10		R75B03		R33C08
25	R78F03		R13A04		R27C12
26	R29F11		R47H03		R74B10
27	R10H09		R91A03		R20G01
28	R67B04		R26F01		R75B03
29	R74B10		R35F02		R93G06
30	R20F10		R50F12		R91A03
31	R77H04		R14F11		R82C10
32	R27E04		R43G02		R70F10
33	R41C06		R66A08		R24H08
34	R86A11		R55E07		R40G12
35	R89D06		R73D06		R18H11
36	R93D10		R65D06		R39H01
37	R58F09		R13B07		R30A05
38	R59H07		R80F03		R50F12
39	R81C04		R88H09		R43G02
40	R50F02		R39D07		R26F01
41	R83C05		R15F08		R53B06
42	R29E02		R82F06		R88F04
43	R59G12		R93D06		R25B07
44	R25B07		R77H04		R94F11
45	R82C10		R31A12		R35G04
46	R32E06		R42B08		R52C09
47	R59H05		R94B04		R47F09
48	R60C05		R26E08		R23A07
49	R88F04		R67B02		R88F03
50	R54B03		R70A05		R32A08

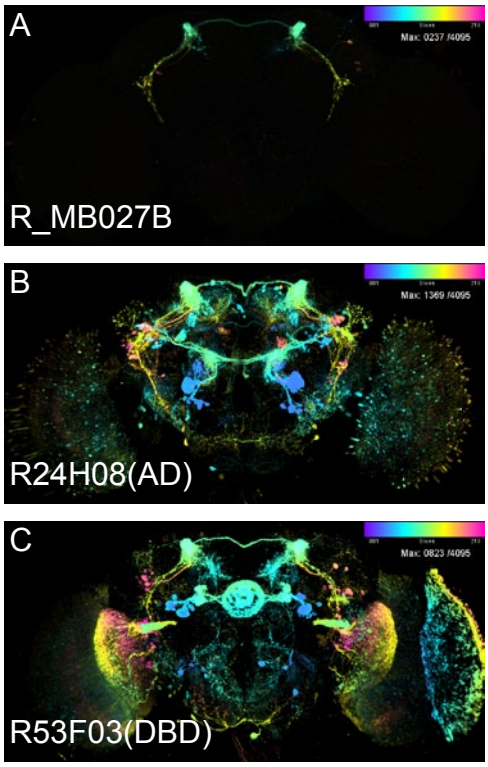

Table 1

R_OL0001B_AD_R64G10_DBD_R35B06

	ColorMIP (32)		N-VFB (5)		N-DSLT (9)
	Line		Line		Line
1	R12H11		R75G12		R84C01
2	R24A08		R37A08		R92C11
3	R52C06		R94B04		R64G10
4	R93E01		R59A05		R24A08
5	R26D04		R70F05		R35B06
6	R20F06		R14A11		R23C12
7	R79A05		R21E05		R20F06
8	R16E01		R89F06		R22H07
9	R70G02		R22H07		R12F01
10	R75G12		R31B05		R59E04
11	R87C07		R64D09		R70G11
12	R24C05		R34E01		R75G12
13	R35B06		R44A01		R84B09
14	R10A11		R26G02		R39H08
15	R13B07		R26A03		R17A04
16	R32E05		R12F01		R13B07
17	R64G10		R35D04		R82D11
18	R24A05		R47H03		R24C10
19	R59G08		R92D04		R37A08
20	R84C12		R46H08		R53H04
21	R23G06		R45F09		R89E02
22	R12D02		R75A10		R49A08
23	R92C11		R67A12		R50D07
24	R67A12		R19G01		R80B12
25	R18D05		R39H08		R21D03
26	R22C04		R86D05		R10H09
27	R91H07		R70D01		R91H07
28	R53E03		R20G09		R59D06
29	R12D12		R41C07		R46H08
30	R32E04		R33C08		R71D07
31	R33C08		R32D03		R41B04
32	R70G11		R65B05		R26G02
33	R12F01		R33B12		R94B04
34	R41B12		R74G08		R70F05
35	R39H12		R22A07		R92D04
36	R22B07		R82D11		R94E06
37	R53D01		R59D06		R91F10
38	R33A12		R71F06		R50A05
39	R42B08		R46G08		R70D01
40	R42F06		R44E11		R53A06
41	R53C04		R71C02		R59A05
42	R84C01		R20G06		R44H11
43	R49A08		R18D04		R72G01
44	R22B05		R71D07		R46F08
45	R85H12		R58E12		R38A12
46	R41B04		R28F07		R47A10
47	R59D06		R24A02		R74G08
48	R55E01		R67E03		R51E08
49	R93B06		R89B06		R93D10
50	R25G04		R74H04		R70A09

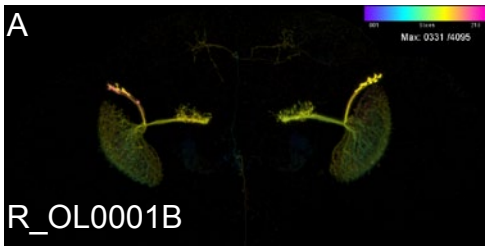

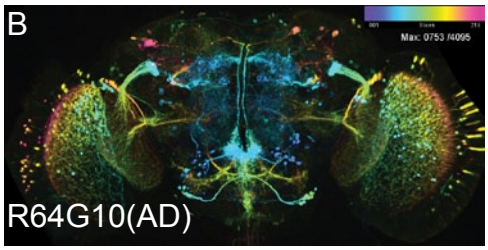

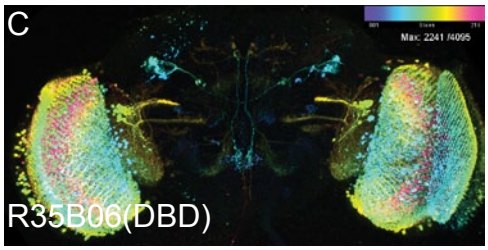

Table 2

R_OL0015B_LC11_AD_R22H02_DBD_R20G06

	ColorMIP (22)		N-VFB (12)		N-DSLT (14)
	Line		Line		Line
1	R92A12		R65B05		R39H08
2	R22H02		R18D04		R24G09
3	R20G06		R34E01		R94H07
4	R54C12		R21E05		R82D11
5	R81D02		R14A11		R14A11
6	R51F09		R64D09		R20G06
7	R14C08		R75G12		R71C02
8	R21F03		R92A08		R70A09
9	R42H07		R20G06		R54C12
10	R70A09		R70F05		R22H02
11	R92A08		R47H03		R50C10
12	R72F08		R59A05		R36B06
13	R87B04		R92G12		R26A03
14	R78G06		R35D04		R51F09
15	R75E11		R39H08		R50D07
16	R92G12		R75A10		R24A02
17	R39H08		R86D05		R75B01
18	R78G03		R22H02		R21D03
19	R65C12		R26A03		R19C05
20	R19D07		R31B05		R46H08
21	R92B11		R21B04		R19G01
22	R47B02		R71D07		R82F11
23	R23D02		R70D01		R31G04
24	R24F08		R47B02		R12F01
25	R36B06		R71C02		R28F07
26	R83B01		R78G03		R92B02
27	R64G09		R54C12		R53H04
28	R21B04		R64G09		R70G11
29	R85D04		R65C12		R72G05
30	R91C11		R70A09		R25G03
31	R24C10		R29E05		R51E07
32	R74H04		R74H04		R47E07
33	R85F11		R89F06		R58D09
34	R12H12		R94B04		R87B04
35	R53F03		R19G01		R35D04
36	R59A12		R80D06		R18D04
37	R50C08		R32D03		R28G03
38	R26F03		R32A08		R31B05
39	R92B02		R13F03		R41C05
40	R64D09		R24C10		R71D07
41	R95A10		R86D04		R24C10
42	R91H06		R28F07		R85F11
43	R47E02		R78G06		R46F08
44	R21D03		R94H07		R49A08
45	R46F08		R37A08		R92A08
46	R25A07		R46F08		R75G12
47	R47H03		R22H07		R80B12
48	R65B04		R92A12		R10C07
49	R20B02		R91C11		R48H05
50	R45G02		R21D03		R72F01

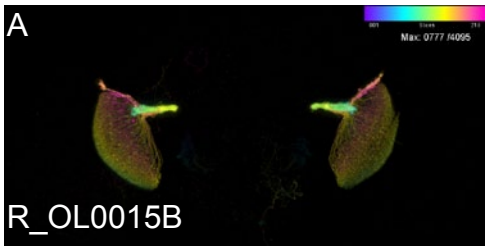

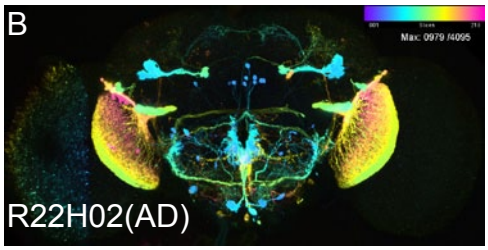

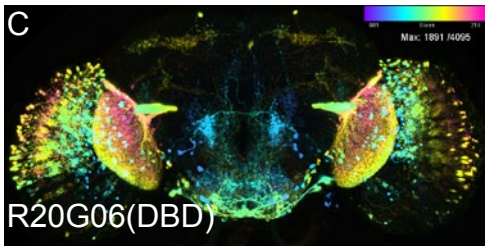

Table 3

SS00732_AD_R14F03_DBD_R24C07

	ColorMIP (7)		N-VFB (4)		N-DSLT (7)
	Line		Line		Line
1	R40H04		R22D06		R78A10
2	R35D10		R39D10		R91H10
3	R36C10		R24C07		R84E03
4	R24C07		R20G01		R35D10
5	R39D10		R92H11		R84F01
6	R66B06		R35D10		R92H11
7	R22C10		R25G04		R22D06
8	R92H11		R14E06		R64G04
9	R22C12		R47H03		R56B12
10	R44E11		R15G04		R93D01
11	R25G04		R60F09		R85A12
12	R21F01		R75F10		R33F11
13	R72F09		R28C04		R21F01
14	R40F11		R10E03		R93C07
15	R95E01		R46G08		R82A06
16	R12D04		R22C12		R40H04
17	R14E05		R95D12		R14F03
18	R49D05		R37A08		R36C02
19	R28F12		R55A10		R91A03
20	R32G09		R40F11		R70D03
21	R92A06		R15E12		R64A07
22	R10B09		R30H09		R60F09
23	R14F03		R22C10		R72H02
24	R93B06		R82H06		R15E12
25	R81B10		R49E03		R92H05
26	R65D09		R32G09		R64A12
27	R58E04		R49A02		R58F06
28	R86B12		R44E11		R39D10
29	R30H05		R50A03		R10E03
30	R60D05		R64B05		R47A10
31	R11A12		R49D05		R76G01
32	R22D06		R50F12		R66A06
33	R52D03		R95E01		R76C04
34	R12F05		R74A06		R70C01
35	R15E12		R20B09		R48B04
36	R66C01		R47F08		R44E11
37	R31G11		R67D01		R22C05
38	R85A12		R47G10		R26F01
39	R83B04		R87E11		R46A02
40	R21H12		R70C01		R82F10
41	R50A03		R16A07		R32A08
42	R56B12		R32A08		R93B10
43	R92G05		R21F01		R68B02
44	R47H03		R19F05		R31H04
45	R74G09		R31H04		R24E12
46	R85F09		R93C07		R64B05
47	R87F08		R88E07		R64F04
48	R50G09		R86F11		R23F06
49	R16H05		R21A10		R69A02
50	R55A10		R86C02		R47H03

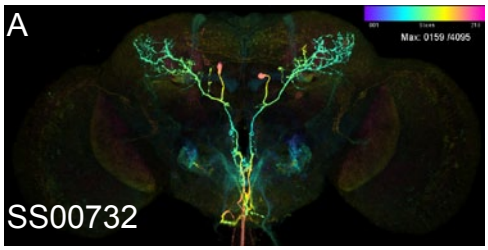

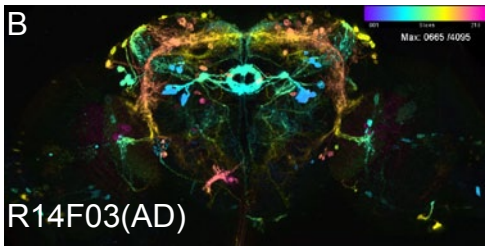

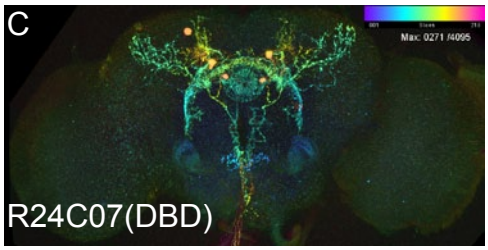

Table 4

SS04159_AD_R59F08_DBD_R47H03

	ColorMIP (7)		N-VFB (2)		N-DSLT (2)
	Line		Line		Line
1	R20A07		R29D12		R83B01
2	R47H03		R11B09		R29G05
3	R47D05		R64E01		R77E11
4	R47F08		R53C11		R35H09
5	R29G05		R32H03		R21C03
6	R60B05		R21C03		R74D04
7	R89H04		R75A10		R69G01
8	R46D02		R83C03		R82F05
9	R13F10		R49G11		R35F02
10	R27B03		R11F08		R59C08
11	R12G12		R31B12		R33H04
12	R21C03		R20A07		R16B05
13	R15F10		R37A08		R71A02
14	R64E01		R80F03		R78F01
15	R69G01		R50E11		R20G01
16	R49A11		R55D07		R47D05
17	R34E01		R27B03		R33D07
18	R41B10		R23H05		R83C03
19	R52H02		R26G02		R72F05
20	R17A07		R72F05		R86E05
21	R41B06		R34C08		R92A12
22	R24C06		R30B01		R30H05
23	R71B04		R34E01		R65A06
24	R22B10		R20G01		R74B08
25	R30C12		R45C07		R80E09
26	R54D07		R21H04		R75A10
27	R58F04		R55B01		R50E11
28	R60D05		R92H11		R93E07
29	R45C07		R53B06		R33D04
30	R30H05		R70H02		R91B09
31	R70H02		R47D05		R49G11
32	R64F05		R33B12		R49C12
33	R77A08		R10A11		R23F03
34	R72G12		R78F01		R52H02
35	R94F06		R44E11		R31E02
36	R95C02		R86D04		R17A07
37	R50D09		R12G12		R85A02
38	R86D04		R94B08		R52C12
39	R53B06		R22B01		R39G05
40	R17A03		R31E02		R87F12
41	R25G03		R38A05		R91F03
42	R58G11		R47F08		R95D12
43	R65C08		R30A09		R33F11
44	R54E02		R24F10		R80G04
45	R23H05		R66A07		R55D07
46	R25G04		R52H02		R83H05
47	R50A08		R47H03		R92H11
48	R26G02		R16G01		R82C10
49	R43C10		R35H09		R50C06
50	R29D12		R52A06		R89H04

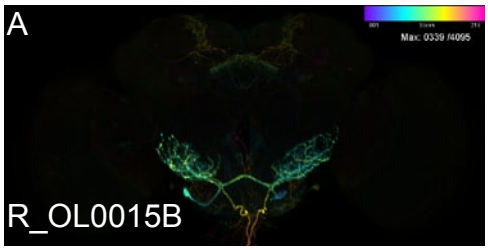

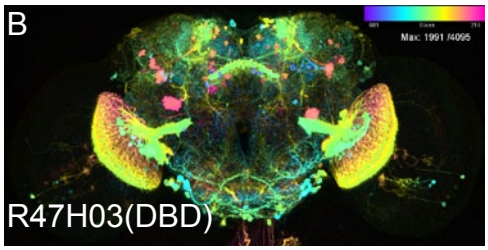

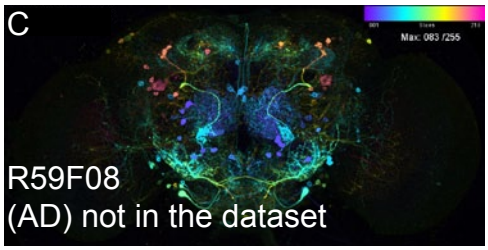

Table 5

R_MB027B_AD_R24H08_DBD_R53F03

Line	C	V	D
R53B06	C#1	V#2	D#43
R42D11	C#2	V#1	-
R53F03	C#4	V#8	D#14
R93G02	C#5	V#7	D#4
R34H05	C#6	V#13	D#3
R24H08	C#7	V#6	D#33
R38D01	C#8	V#4	-
R33E02	C#9	V#5	D#10
R92B01	C#14	-	-
R93G06	C#18	V#11	D#29
R49A11	C#20	V#3	-
R81E11	C#22	-	-
R78F03	C#25	V#13	-
R74B10	C#29	V#9	D#26
R89D06	C#35	V#19	-
R29E02	C#42	-	-
R25B07	C#44	-	D#43

Table 6

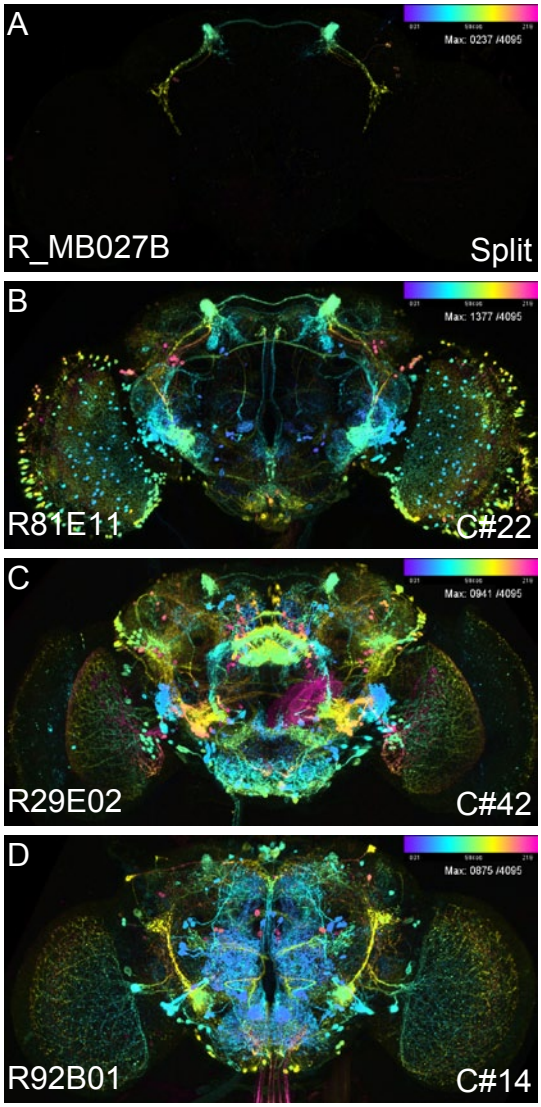

R_OL0001B_AD_R64G10_DBD_R35B06

Line	C	V	D
R12H11	C#1	-	-
R24A08	C#2	-	D#4
R52C06	C#3	-	-
R93E01	C#4	-	-
R26D04	C#5	-	-
R20F06	C#6	-	D#7
R79A05	C#7	-	-
R16E01	C#8	-	-
R70G02	C#09	-	-
R87C07	C#11	-	-
R24C05	C#12	-	-
R35B06	C#13	-	D#5
R10A11	C#14	-	-
R13B07	C#15	-	D#16
R64G10	C#17	-	D#3
R24A05	C#18	-	-
R59G08	C#19	-	-
R84C12	C#20	-	-
R67A12	C#24	V#23	-
R18D05	C#25	-	-
R22C04	C#26	-	-
R91H07	C#27	-	-
R12D12	C#29	-	-
R32E04	C#30	-	-
R33C08	C#31	V#30	-
R70G11	C#32	-	D#11
R53D01	C#37	-	-
R42B08	C#39	-	-
R84C01	C#42	-	D#1
R49A08	C#43	-	-
R22B05	C#44	-	-
R55E01	C#48	-	-
R31B05	-	V#10	-
R37A08	-	V#2	D#19
R74H04	-	V#50	-
R92C11	-	-	D#2

Table 7

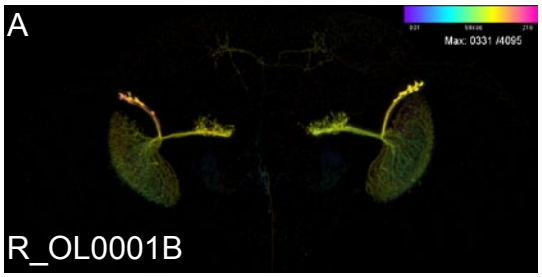

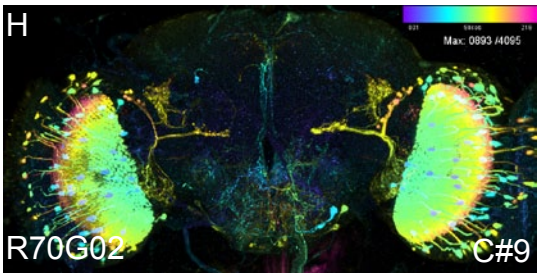

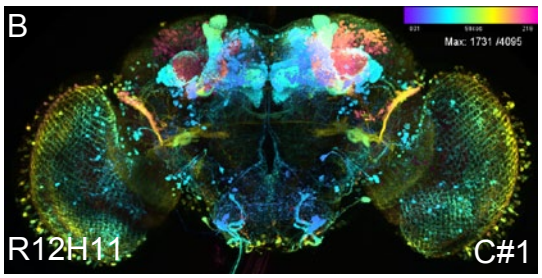

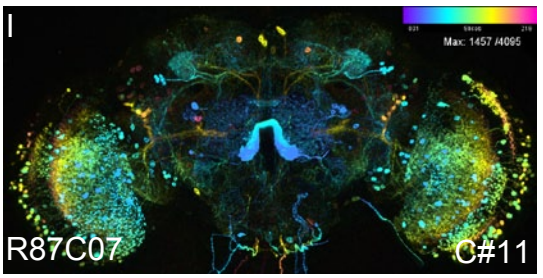

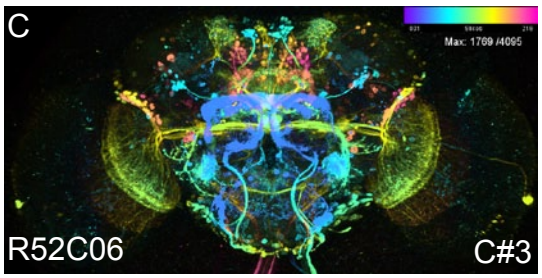

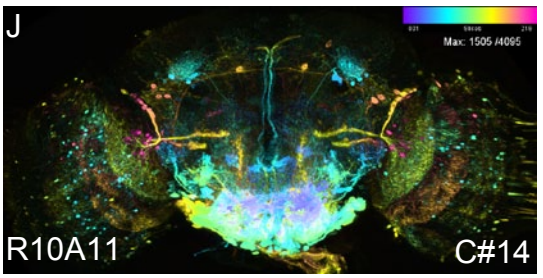

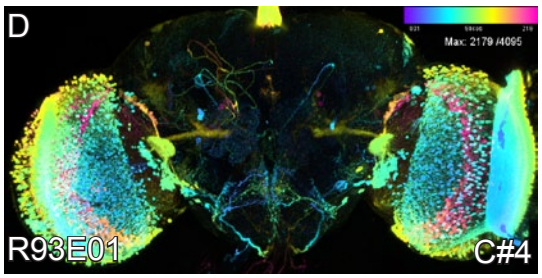

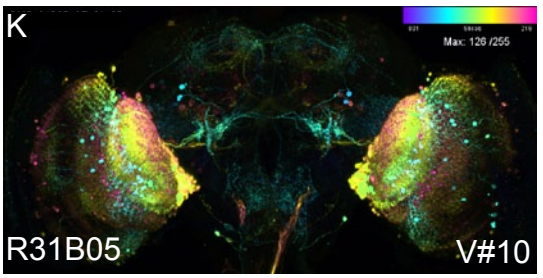

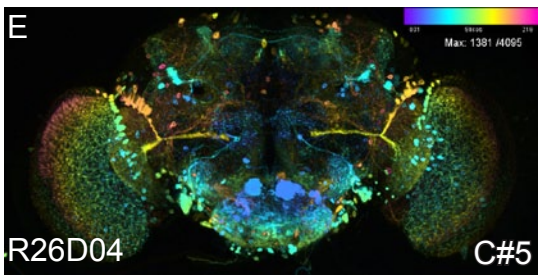

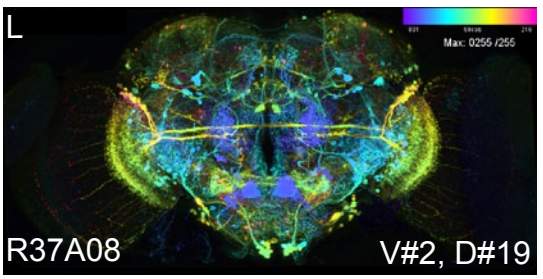

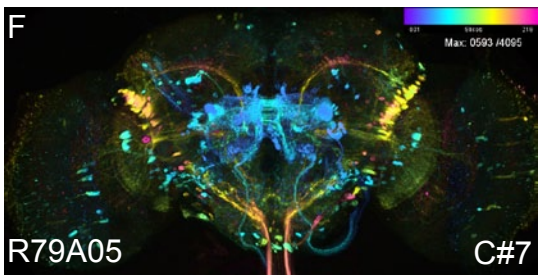

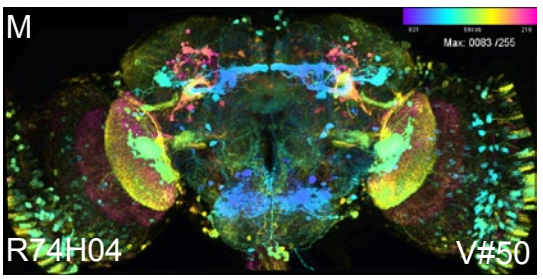

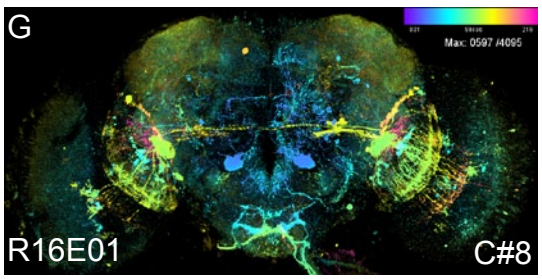

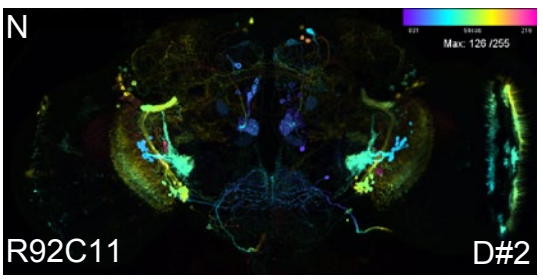

R_OL0015B_LC11_AD_R22H02_DBD_R20G06

Line	C	V	D
R92A12	C#1	V#48	
R22H02	C#2	V#20	D#10
R20G06	C#3	V#9	D#6
R54C12	C#4	V#27	D#9
R81D02	C#5	-	-
R51F09	C#6	-	D#14
R14C08	C#7	-	-
R92A08	C#11	V#8	D#45
R72F08	C#12	-	-
R87B04	C#13	-	D#34
R19D07	C#20	-	-
R47B02	C#22	V#24	-
R23D02	C#23	-	-
R83B01	C#26	-	-
R85D04	C#29	-	-
R91C11	C#30	V#49	-
R85F11	C#33	-	D#42
R12H12	C#34	-	-
R53F03	C#35	-	-
R59A12	C#36	-	-
R92B02	C#39	-	D#26
R25A07	C#46	-	-
R18D04	-	V#2	D#36
R47E07	-	-	D#32
R71C02	-	-	D#7
R75A10	-	V#16	-
R75B01	-	-	D#17
R80D06	-	V#36	-
R89F06	-	V#33	-
R94H07	-	V#44	D#3

Table 8

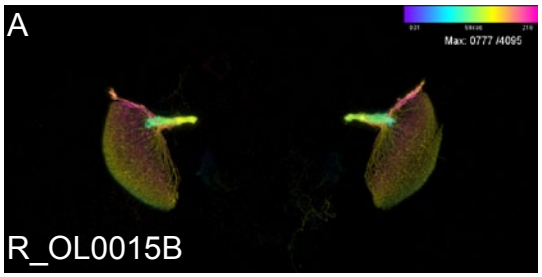

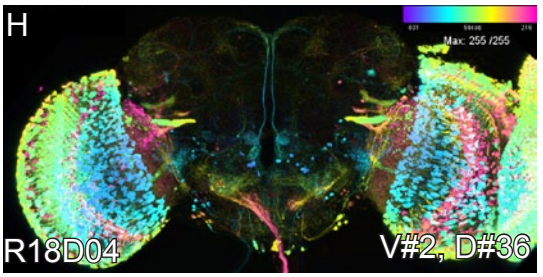

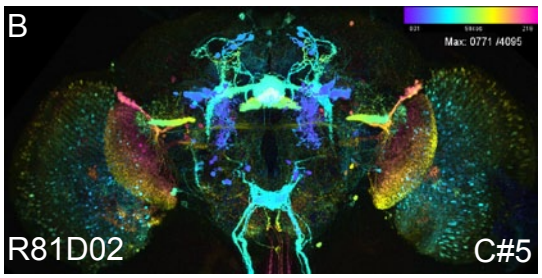

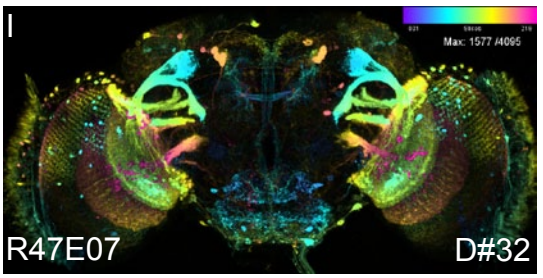

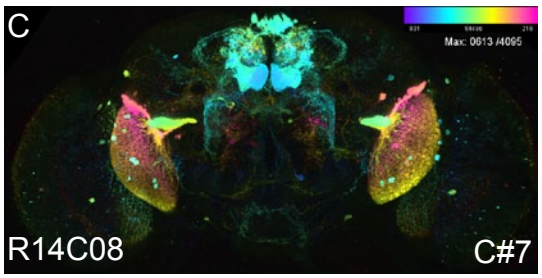

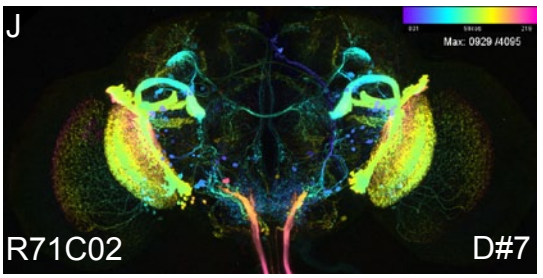

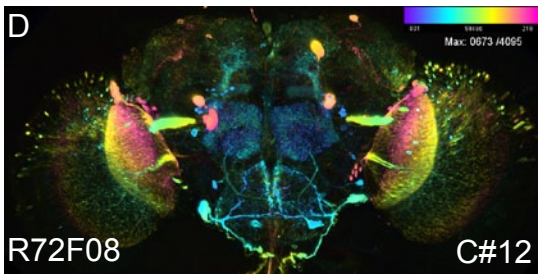

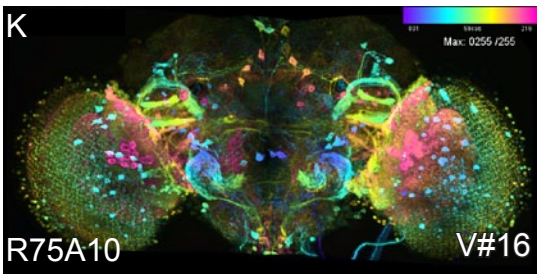

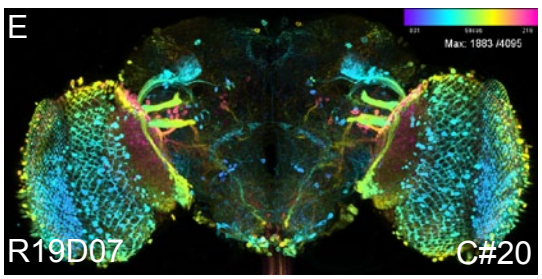

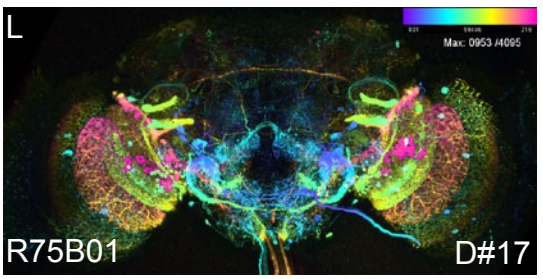

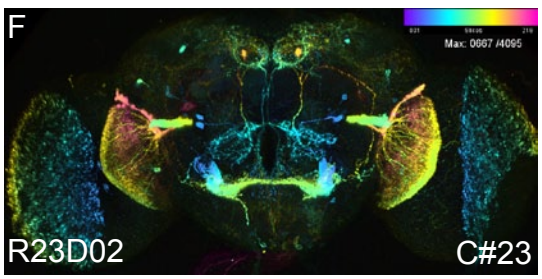

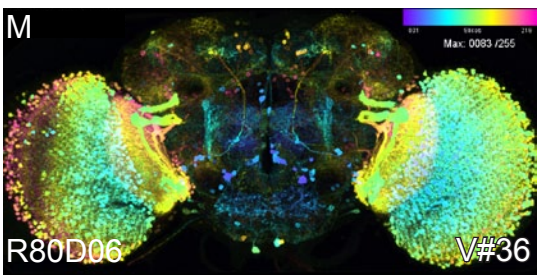

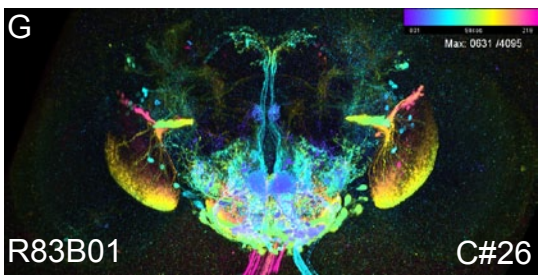

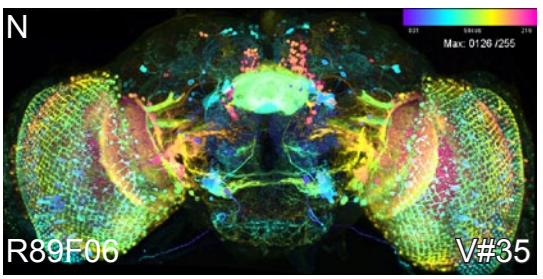

SS00732_AD_R14F03_DBD_R24C07

Line	C	V	D
R40H04	C#1	-	D#16
R35D10	C#2	V#8	D#4
R24C07	C#4	V#3	-
R39D10	C#5	V#2	D#30
R14F03	C#23	-	D#17
R22D06	C#32	V#1	D#7
R85A12	C#38	-	D#11
R84E03	-	-	D#3

Table 9

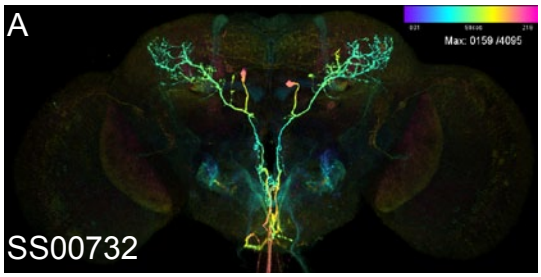

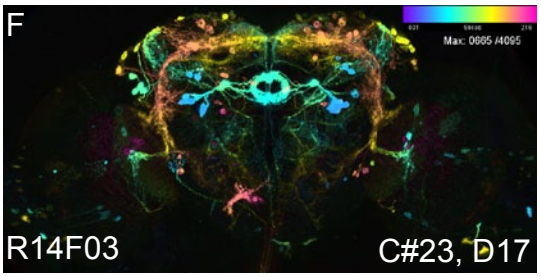

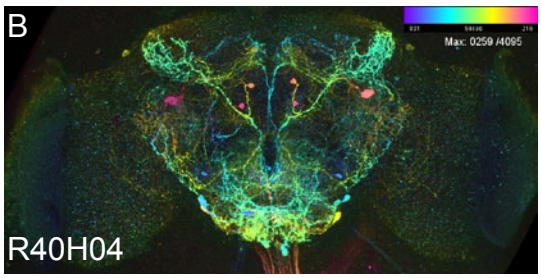

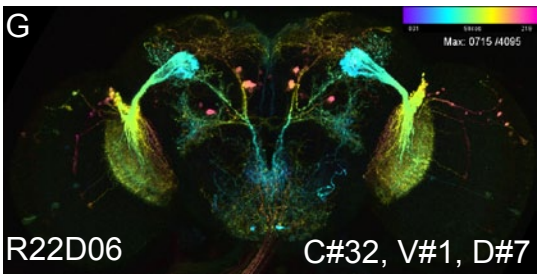

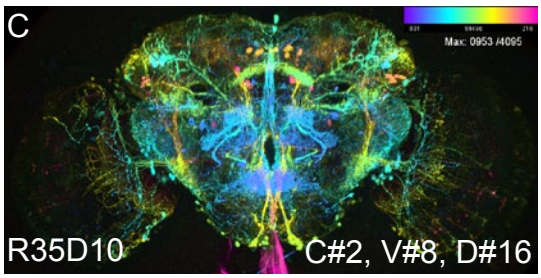

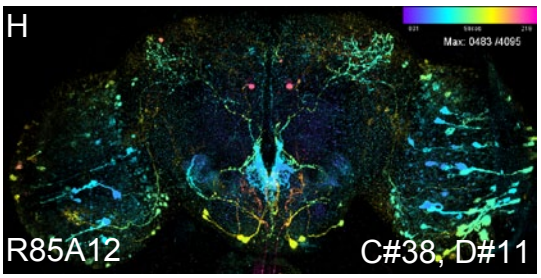

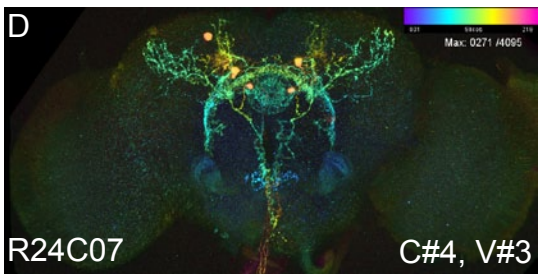

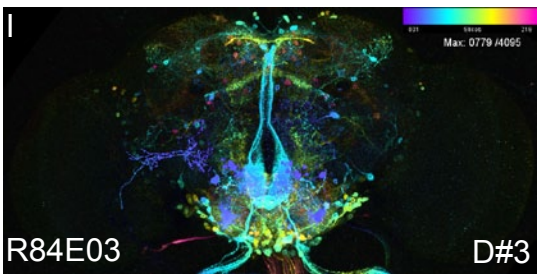

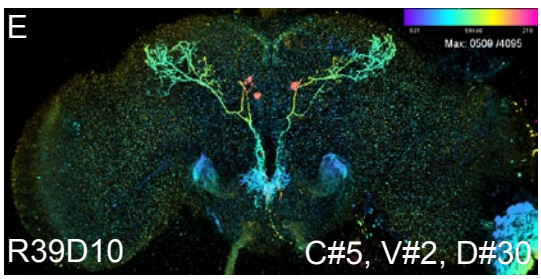

SS04159_AD_R59F08_DBD_R47H03

Line	C	V	D
R47H03	C#2	V#47	-
R49A11	C#16	-	-
R22B10	C#24	-	-
R70H02	C#31	V#30	-
R95C02	C#36	-	-
R50A08	C#47	-	-
R92A12	-	-	D#21
R65A06	-	-	D#23

Table 10